Advanced Course on Structural Control and Health Monitoring
SMART'01 – (pp.109–122) – Warsaw, May 22-25, 2001.

Dynamics of cracked and delaminated composite material structures

W.M. OSTACHOWICZ and M. KRAWCZUK

Polish Academy of Sciences, Institute of Fluid Flow Machinery
ul. Gen. J. Fiszera 14, 80-952 Gdańsk, Poland

Dynamic response measurements are a very attractive form of damage detection tests since they can be made at a single point on the component and are independent of the position chosen. The aim of this paper is to present investigations, to enable the analysis of the influence of the fatigue cracks and delaminations on the dynamic characteristics of the constructions made of unidirectional composite materials. The method of modelling the crack or delamination presented in the paper enables an easy modification of the investigated elements according to their specific damage (oblique crack, two-side crack, inside crack, multiple delaminations, etc.). The numerical examples are in consistence with the known influence of the position and depth of the crack on the decrease of the natural bending frequencies of structures. Simultaneously, a strong influence of the material parameters on these changes has been observed, which does not exist in the case of isotropic materials.

1. Introduction

The use of composite materials in various construction elements has increased substantially over the past few years. These materials are particularly widely used in situations where a large strength-to-weight ratio is required. Similarly to isotropic materials, composite materials are subjected to various types of damage, mostly cracks and delaminations. These result in local changes of the stiffness of elements from such materials and consequently their dynamic characteristics are altered. This problem is well understood in the case of construction elements made from isotropic materials, while data concerning the influence of fatigue cracks on the dynamics of composite construction elements are scarce in the available literature.

The aim of the work presented in this paper is to analyse the influence of a fatigue crack and delamination on the changes in the dynamics of structures made of composite materials. This problem has been solved by using the finite element method. The damaged part of the structures has been modelled by special finite elements with failures, while the undamaged parts have been represented by other, well known finite elements. The influence of material parameters (fibre angle and volume of the fibre) on the intensity of the changes is also investigated.

2. Cracked, unidirectional composite beam

Damage models in composite structures have been studied extensively by many researchers. Krawczuk, Ostachowicz, and Żak proposed [1, 2] the formulation of a finite composite beam element with an open crack. The damaged part of the beam has been modelled by a special finite element with a crack (Fig. 1), while the undamaged parts have been modelled using three-noded beam elements. The crack is placed in the middle of the element and remains open, its depth being a. The angle between the fibre and the axis of the element is α. The element has three nodes. Each of them has two degrees of freedom, in the form of transverse displacements and rotations. In paper [1] only the case of pure bending was considered. Assuming that there is no warping in the transverse cross-section of the element, the displacements on both sides of the element can be expressed by:

$$\begin{cases} u_{x1}(x,y) = -y\,\phi_1(x), \\ u_{y1}(x,y) = v_1(x), \end{cases} \qquad \begin{cases} u_{x2}(x,y) = -y\,\phi_2(x), \\ u_{y2}(x,y) = v_2(x), \end{cases} \tag{1}$$

where ϕ_i $(i = 1, 2)$ denotes rotation and v_i $(i = 1, 2)$ denotes transverse displacements. Transverse displacements v_i on both sides of the crack can be approximated by cubic polynomials while the independent rotations ϕ_i can be approximated by quadratic polynomials [1, 2].

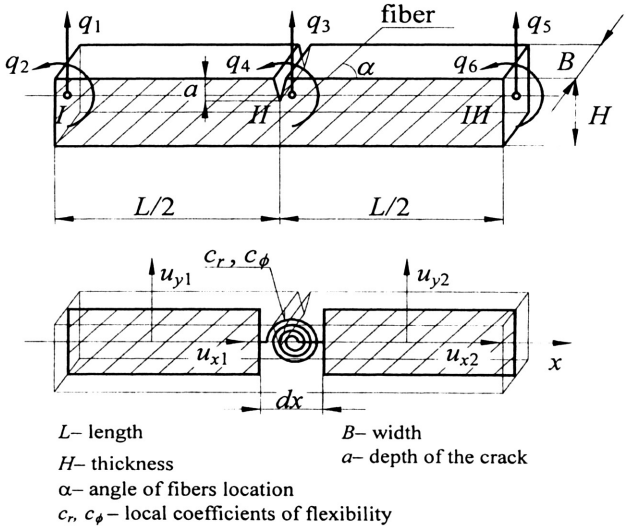

FIGURE 1. A composite beam finite element with a transverse crack.

By using the conditions in the nodes of the element and the conditions expressing consistency of displacements in the x and y directions, and the balance of forces and torque (2) we can formulate a stiffness matrix for the finite elements.

$$\begin{cases} v_1(0) = q_1, \\ \phi_1(0) = q_2, \\ v_1(L/2) = q_3, \\ \phi_1(L/2) = q_4, \\ v_2(L) = q_5, \\ \phi_2(L) = q_6, \end{cases} \quad \begin{cases} u_{x1}(L/2) - u_{x2}(L/2) = c_r\, u'_{x1}(L/2), \\ u'_{x1}(L/2) = u'_{x2}(L/2), \\ u_{y1}(L/2) = u_{y2}(L/2), \\ u'_{y1}(L/2) - u'_{y2}(L/2) = c_\phi\, u''_{y1}(L/2), \\ u''_{y1}(L/2) = u''_{y2}(L/2), \\ u'''_{y1}(L/2) = u'''_{y2}(L/2). \end{cases} \tag{2}$$

Values c_r and c_ϕ in Eqs. (2) represent the flexibility coefficients of the element in the crack. The flexibility coefficients of the element due to the appearance of the crack can be obtained from the Castigliano theorem i.e.:

$$c_{ij} = \frac{\partial^2 U}{\partial P_i \partial P_j}, \tag{3}$$

where U is the additional elastic strain energy of the element caused by the crack, and P_i and P_j denote independent nodal forces of the finite element. We can calculate this additional elastic strain energy in the case of cracks existing in unidirectional composite materials (Nikpour and Dimarogonas, [3]) from the following formula:

$$U = \int_A \left\{ D_1 \sum_{i=1}^{n} K_{Ii}^2 + D_{12} \sum_{i=1}^{n} K_{Ii} \sum_{j=1}^{n} K_{IIj} + D_2 \sum_{i=1}^{n} K_{IIi}^2 \right\} dA, \tag{4}$$

where A is the surface of the crack, K_{Ii} and K_{IIi} $(i, j = 1, 2, \ldots, n)$ are stress intensity factors for the i-th independent nodal force of the element, and D_1, D_{12}, D_2 are coefficients depending on the material parameters (Nikpour, [4]). According to the results presented by Bao et al. [5] these factors may be written as:

$$K_{ji} = \sigma_i \sqrt{\pi\, a}\, F_{ji}(a/H) Y_j(\varsigma), \tag{5}$$

where σ_i denotes the stress acting in the crack, a is the depth of the crack, H is the height of the element, F_{ji} are correction factors, which consider the finite dimensions of the element and also properties of the material while $Y_j(\zeta)$ is a correction function which takes into account the anisotropy of the material. Details of their formulation one cans find in [1].

3. Natural vibration of a cantilever composite beam with a crack

Examples of numerical calculations showing the influence of crack parameters (depth and position) and material parameters (fibre volume fraction and fibre angle) on the changes of the frequency of natural bending vibrations were carried out for a cantilever beam, the geometrical dimensions of which are shown in Fig. 2.

It has been assumed that the beam is made of unidirectional composite material (graphite fibre-reinforced polyamide). Material parameters of the components, and relationships to calculate the gross material coefficients for the composite material analysed, are presented in Table 1.

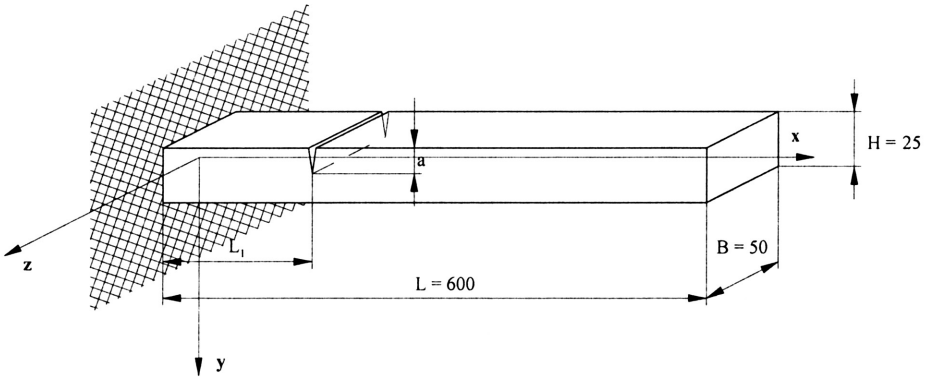

FIGURE 2. Composite cantilever beam.

TABLE 1. Properties of graphite fibre-reinforced polyamide composite

	Matrix (epoxy resin)	Fibres (graphite)
Young's modulus [GPa]	$E_m = 3.43$	$E_f = 275.6$
Poisson ratio	$\nu_m = 0.35$	$\nu_f = 0.2$
Density [kg/m^3]	$rho_m = 1250$	$\rho_f = 1900$

In Figs. 3–5 results are given showing the influence of the position and depth of the crack on the first three natural frequencies of the analysed beam. The beam was modelled by 10 finite elements.

Numerical calculations have been carried out by assuming the overall volume of fibres to be 30% and the fibre angle to be 30° (measured between the geometric axis of the beam and the material's principal axes).

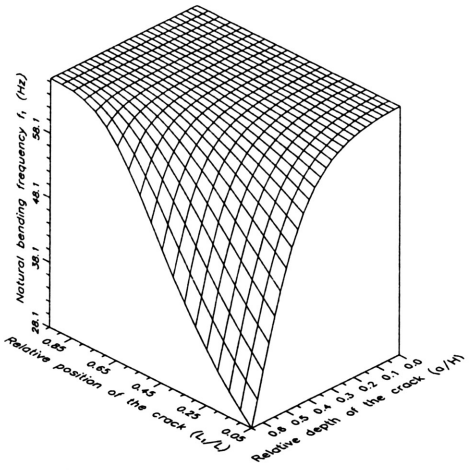

FIGURE 3. First natural bending frequency versus depth and location of the crack.

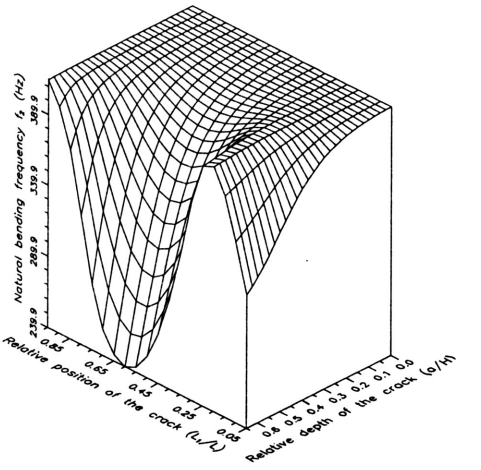

FIGURE 4. Second natural bending frequency versus depth and location of the crack.

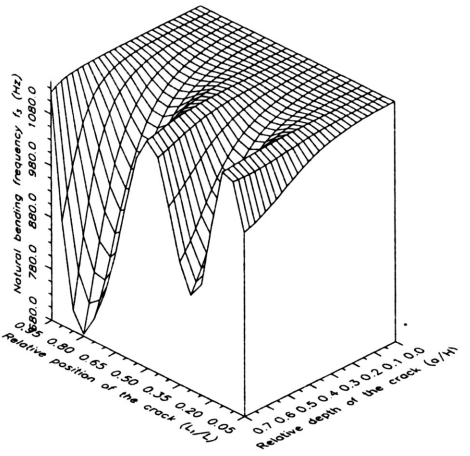

FIGURE 5. Third natural bending frequency versus depth and location of the crack.

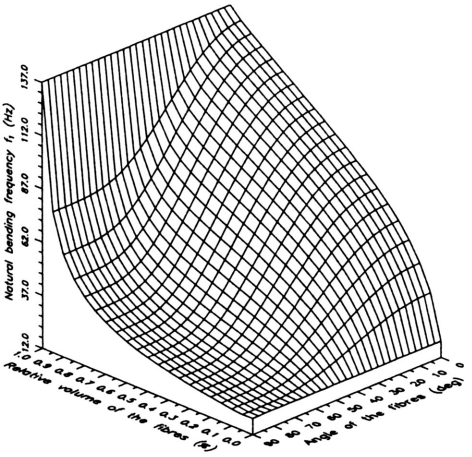

FIGURE 6. First natural bending frequency versus angle and volume of fibres.

In Fig. 6 the influence of material parameters on the first natural frequency is presented. The relative depth of the crack is 0.4 and the crack is located relatively at 0.25 of the total beam length.

4. Delaminated composite beam

Delamination is one of the most important failure modes in laminated composite materials. Acquired during the manufacturing process, or produced by impact and other service hazards, delamination may greatly reduce the stiffness of the whole structure, thus influencing the vibration and stability characteristics.

This chapter is devoted to the analysis of natural vibrations of a layered composite beam with a single delamination. The beam is modelled by beam finite elements with three nodes, and three degrees of freedom at each node. In the delaminated region, additional boundary conditions are applied. It is assumed that the delamination is open (i.e., damping caused by contact forces between the lower and upper parts can be neglected in the model due to its small influence on the changes of natural frequencies) and extends to the full width of the beam.

In Fig. 7, a model of a delaminated part of the beam is presented (see Krawczuk, Ostachowicz, and Żak [6, 7]) The delaminated region is modelled by three beam finite elements which are connected at the delamination crack tip where additional boundary conditions are applied. The layers are located symmetrically with respect to the $x - z$ plane. The element has three nodes with three degrees of freedom at each node i.e. axial displacement q_1, q_4, q_7, transverse displacement q_3, q_6, q_9, and the independent rotation q_2, q_5, q_8. It has also been assumed that the total number of degrees of freedom in the element is independent of the number of material layers. Neglecting warping, the displacements u and v within a layer can be expressed as:

$$\begin{cases} u(x,y) = u^0(x) - y\,\phi(x), \\ v(x,y) = v^0(x), \end{cases} \tag{6}$$

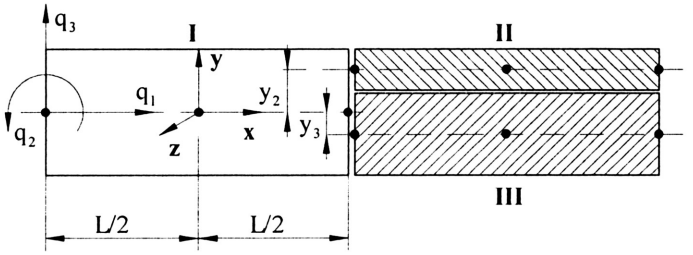

FIGURE 7. Delamination of a beam modelled by finite elements.

where $u^0(x)$ denotes the axial displacements, $\phi(x)$ the independent rotations, and $v^0(x)$ the transverse displacements. The displacements and rotation in the element are clearly formulated in the paper [3].

In order to connect element *I* with elements *II* and *III*, the following boundary conditions are applied at the delamination crack tip:

$$\begin{cases} \phi_1(x) = \phi_2(x) = \phi_3(x), \\ v_1^0(x) = v_2^0(x) = v_3^0(x), \end{cases} \qquad \begin{cases} u_1^0(x) - y_2\,\phi_2(x) = u_2^0(x), \\ u_1^0(x) - y_3\,\phi_3(x) = u_3^0(x), \end{cases} \tag{7}$$

where y_2 and y_3 denotes distances between the neutral axes of elements *I-II* and *I-III*, respectively (see Fig. 7).

In the finite-element modelling the cubic polynomial in x was taken to approximate the bending displacement $v^0(x)$, while for the axial displacement $u^0(x)$, and the rotation $\phi(x)$, quadratic polynomials in x were taken. Moreover, it was assumed that the shear strain variation was linear, as proposed by Tessler and Dong [8]. The above conditions enable us the displacements and rotation in the element to be written in the form:

$$\begin{cases} u^0(x) = a_1 + a_2\,x + a_3\,x^2, \\ \phi\,(x) = a_4 + a_5\,x + 3\,a_9\,x^2, \\ v^0(x) = a_6 + a_7\,x + a_8\,x^2 + a_9\,x^3, \end{cases} \tag{8}$$

Using these conditions at the nodes of the element the unknown coefficients, a_1–a_9, can be easily determined as a function of the nodal displacements. Then the matrix of the shape functions for a single layer of the element can be calculated.

The strains within a single material layer are given by the following formula:

$$\begin{cases} \varepsilon_x = \dfrac{\partial u\,(x,y)}{\partial x} = \dfrac{\partial u^0\,(x)}{\partial x} - y\,\dfrac{\partial \phi\,(x)}{\partial x}, \\ \gamma_{xy} = \dfrac{\partial u\,(x,y)}{\partial y} + \dfrac{\partial v\,(x,y)}{\partial x} = \dfrac{\partial v^0\,(x)}{\partial x} - \phi\,(x). \end{cases} \tag{9}$$

The calculated constants, a_1–a_9, and relations (8) and (9) allow the calculation of the strain-displacement matrix of the material layer and then from that the stiffness matrix of the material layer can be evaluated. The inertia matrix and the stiffness matrix for the whole element can be calculated using the formulae:

$$M_e = \sum_{j-1}^{R} M_e^j = \sum_{j-1}^{R} \rho_j \int_{V_i} N^T N \, dV_j, \tag{10}$$

$$K_e = \sum_{j-1}^{R} K_e^j = \sum_{j-1}^{R} \int_{V_i} B^T D_j B \, dV_j, \tag{11}$$

where j is the number of the layer, R the global number of the layers in the element, V_j the volume of the j-th layer, and ρ_j the density of the j-th layer while D_j is the stress–strain relations matrix for the j-th layer.

5. Natural vibration of a cantilever composite beam with a delamination

Numerical tests were performed for a cantilever beam presented in Fig. 8. The beam was manufactured from 24 layers of graphite-epoxy resin composite material (see Table 1). The volume fraction of graphite fibres in the analysed beam remained constant at 20%. The angle of the fibres in the layers was ±45°. In each layer the fibres were located parallel to the axis of the beam (see Fig. 7).

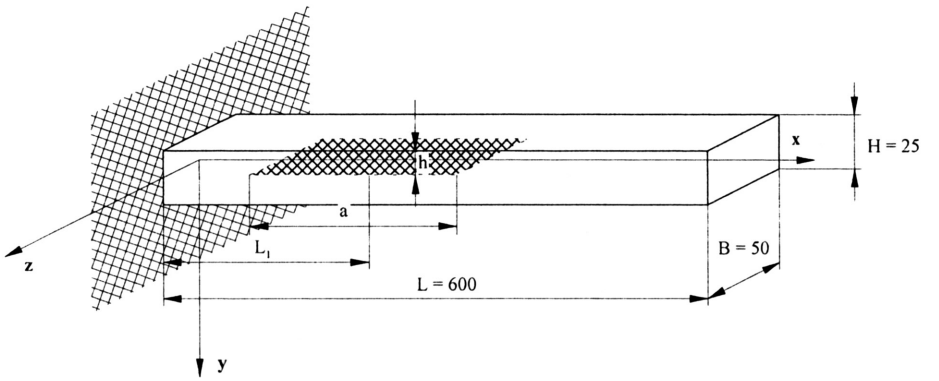

FIGURE 8. Dimensions of the delaminated layered composite beam.

In order to analyse the influence of the position of the delamination the beam was modelled by 18 finite elements, and the relative length of delamination was 6.25%.

In Fig. 9, the influence is shown of the relative delamination position along the beam thickness on the first natural frequency. Figures 10–11 show the influence of the relative delamination position in the x direction on the first and second natural frequency of the layered composite beam.

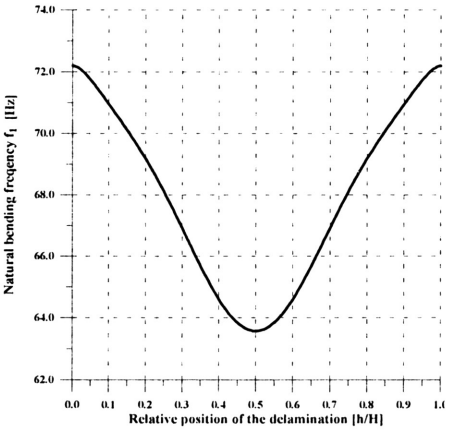

FIGURE 9. First natural bending frequency versus relative position of the delamination.

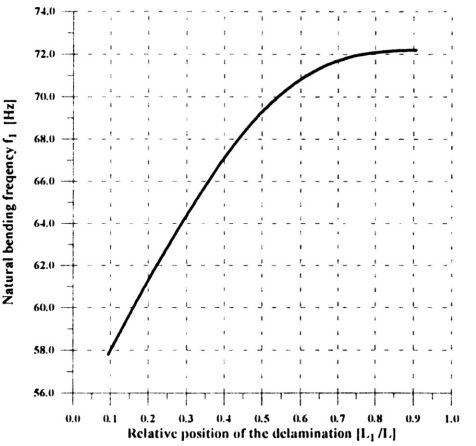

FIGURE 10. First natural bending frequency versus relative position of the delamination.

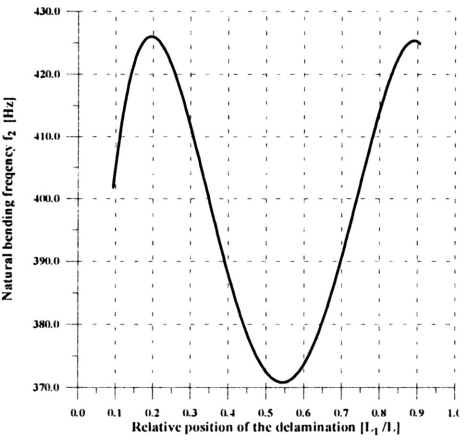

FIGURE 11. Second natural bending frequency versus relative position of the delamination.

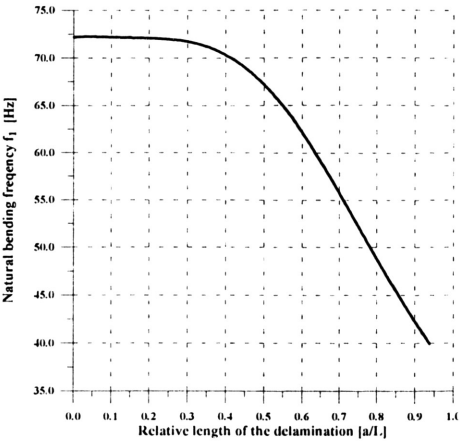

FIGURE 12. First natural bending frequency versus relative length of the delamination.

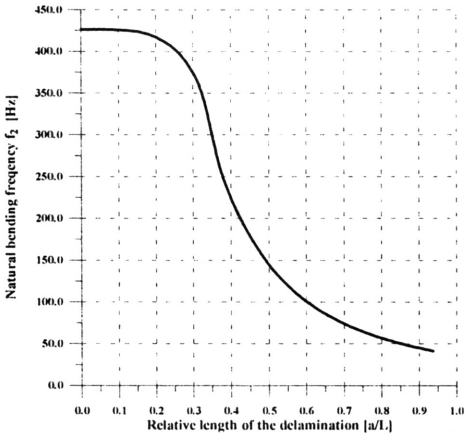

FIGURE 13. Second natural bending frequency versus relative length of the delamination.

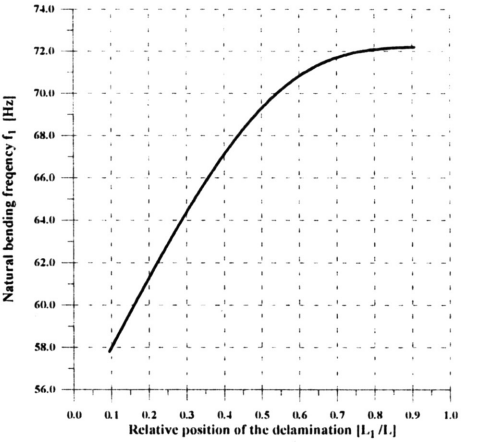

FIGURE 14. First natural bending frequency versus relative position of the delamination.

6. Delaminated composite plate

Figure 15 presents a way of modelling the delaminated region in a composite plate with a delamination. The delamination is modelled by three plate finite elements, and to connect them, additional boundary conditions are applied at the delamination front. The material layers in the elements are located symmetrically with respect to the $x - y$ plane. Each element has eight nodes with five degrees of freedom.

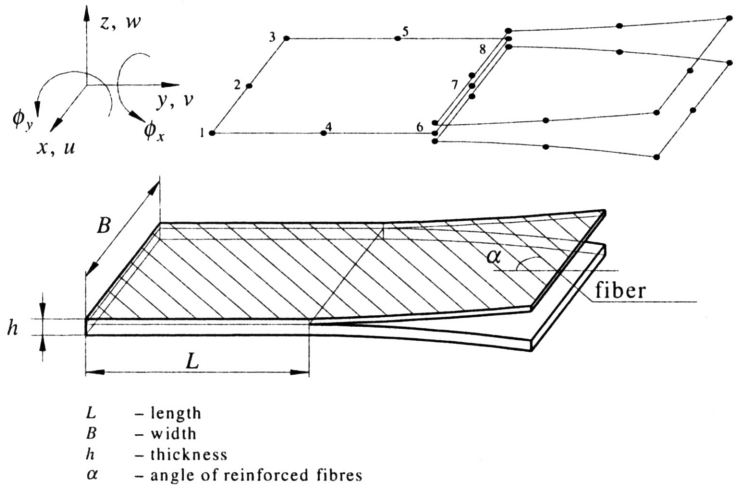

FIGURE 15. The multilayer composite plate with delamination.

The axial displacements u, v and w in a single layer can be expressed by:

$$\begin{cases} u(x,y,z) = u^0(x,y) - z\,\phi_x(x,y), \\ v(x,y,z) = v^0(x,y) - z\,\phi_y(x,y), \\ w(x,y,z) = w^0(x,y), \end{cases} \tag{12}$$

where $u^0(x,y)$, $v^0(x,y)$, and $w^0(x,y)$ denote mid-plane displacements, while $\phi_x(x,y)$ and $\phi_y(x,y)$ denote independent rotations.

To approximate the axial mid-plane displacements and rotations biquadratic shape functions for the eight-node element have been used.

The strains in a single material layer can be calculated from the following relations:

$$\varepsilon_x = \varepsilon_x^0 + z\,\kappa_x = \frac{\partial u^0}{\partial x} - z\frac{\partial \phi_x}{\partial x} \tag{13}$$

The inertia and stiffness matrices for the whole element can be expressed as the sums of the inertia, or stiffness, matrices, of the various single layers:

$$M_e = \sum_{j=1}^{R} M_e^j = \sum_{j=1}^{R} \rho_j \int_{V_j} N^T N\, dV_j, \tag{14}$$

$$K_e = \sum_{j=1}^{R} K_e^j = \sum_{j=1}^{R} \int_{V_j} B^T D_j B\, dV_j, \tag{15}$$

where j is the number of the layers, R the total number of layers in the element, V_j the volume of the j-th layer, and ρ_j the density of the j-th layer, while D_j denotes the stress–strain relations matrix for the j-th layer.

In order to connect the three elements depicted in Fig. 15, and to satisfy continuity of the displacements between these elements, the following boundary conditions were applied at the tip of the delamination:

$$\begin{cases} u_1^0 = u_2^0 + z_2\,\phi_x, \\ u_1^0 = u_3^0 + z_3\,\phi_y, \end{cases} \qquad \begin{cases} v_1^0 = v_2^0 + z_2\,\phi_y, \\ v_1^0 = v_3^0 + z_3\,\phi_y, \end{cases} \tag{16}$$

where z_2 and z_3 denote distances between the neutral axes of elements 1-2 and 1-3, respectively (see Fig. 16).

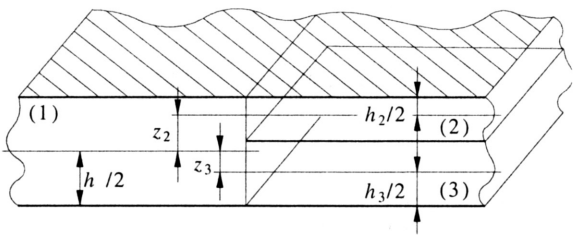

FIGURE 16. The multilayer composite plate with delamination.

7. Natural vibration of a cantilever composite plate with a delamination

The numerical tests were performed for a cantilever plate presented in Fig. 17. The plate was manufactured from 8 layers of graphite-epoxy resin composite material (see Table 2). The volume fraction of graphite fibres in the analysed beam remained constant in the range 20%.

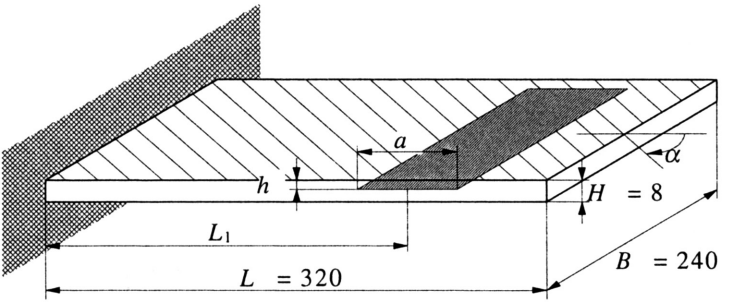

L length
B width
H thickness
a delamination (length)
L_1 delamination (middle point)
h delamination (location between layers)
α angle of reinforced fibres

FIGURE 17. Dimensions of the delaminated layered composite plate.

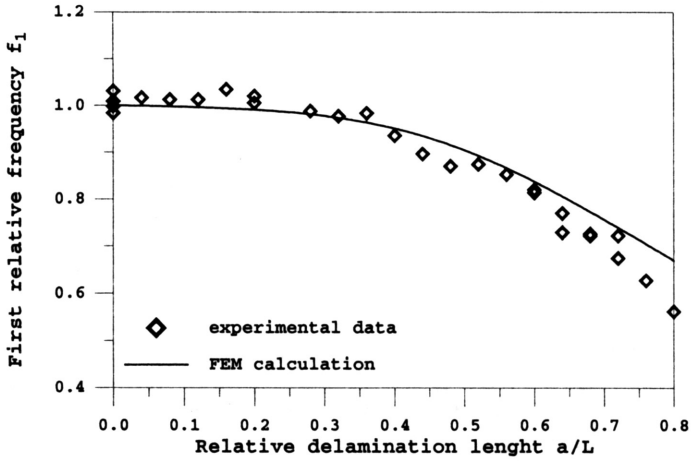

FIGURE 18. Changes in the fundamental natural frequency in bending for the delaminated composite cantilever plate.

TABLE 2. Properties of glass fibre-reinforced epoxy composite

	Matrix (epoxy)	Fibres (glass)
Young's modulus [GPa]	$E_m = 3.43$	$E_f = 66.5$
Kirchhoff modulus [GPa]	$G_m = 1.27$	$G_f = 27.0$
Poisson ratio	$\nu_m = 0.35$	$\nu_f = 0.23$
Density [kg/m^3]	$\rho_m = 1250$	$\rho_f = 2250$

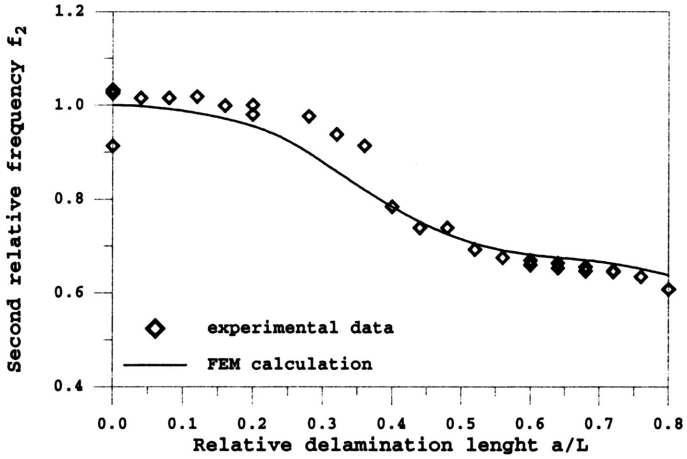

FIGURE 19. Changes in the second bending natural frequency of delaminated composite cantilever plates.

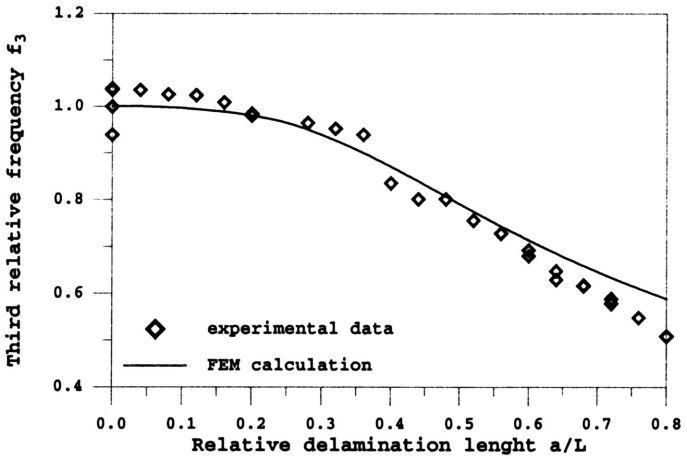

FIGURE 20. Changes in the third bending natural frequency of delaminated composite cantilever plates.

Figure 18 shows the changes in the first bending frequency of the composite plate as a function of the delamination length. Figure 19 illustrates the changes in the second natural frequency, while in Fig. 20 the changes in the third natural frequency are depicted. From Figs.18–20 it arises that the results obtained from numerical calculations are in agreement with the experimental investigation.

8. Conclusions

In this paper a number of typical models of cracked and delaminated structures have been described. There are many challenges in the development of models of structural stiffness loss due to damage. Typical ones are the ability to identify minor changes in the stiffness of composite structures.

Based on the numerical and experimental results presented in the paper the following conclusions can be drawn:

- delaminations in beams and plates result in a decrease in the natural bending frequencies,
- the changes in natural frequencies are functions of the length of the delamination and also on the vibration mode,
- when the size of the failure increases (i.e. the length of the delamination) the reduction in the natural frequencies also increases.

Analytical methods to predict changes in the stiffness parameters are of dubious worth in more complex structures. The difficulties lie in the sort of restrictions described in detail in [9-13]. So far, FEM-based methods have been shown to be more realistic for applications to engineering constructions.

Laboratory experiments are often conducted to ensure the validity of analytical and numerical models. Therefore, a large amount of verification work is still required in order to be able develop practical and effective stiffness detection methods confidently.

References

1. M. KRAWCZUK, W. OSTACHOWICZ and A. ŻAK, *Modal Analysis of Cracked, Unidirectional Composite Beam*, Composites Part B, Vol.28B, pp.641-650, 1997.
2. M. KRAWCZUK and W. OSTACHOWICZ, *Modelling and Vibration Analysis of a Cantilever Composite Beam with a Transverse Open Crack*, Journal of Sound and Vibration, Vol.183, No.1, pp.69-89, 1995.
3. K. NIKPOUR and A.D. DIMAROGONAS, *Local Compliance of Composite Cracked Bodies*, Journal of Composite Science and Technology, Vol.32, pp.209-223, 1988.
4. K. NIKPOUR, *Buckling of Cracked Composite Columns*, International Journal of Solids and Structures, Vol.26, pp.1371-1386, 1990.
5. S. BAO, Z. HO and B. FAN SUO, *The Role of Material Orthotropy in Fracture Specimens for Composites*, International Journal of Solid and Structures, Vol.29, pp.1105-1116, 1992.
6. M. KRAWCZUK, W. OSTACHOWICZ and A. ŻAK, *Natural Vibration Frequencies of Delaminated Composite Beams*, Computer Assisted Mechanics and Engineering Sciences, Vol.3, pp.233-243, 1996.
7. M. KRAWCZUK, W. OSTACHOWICZ and A. ŻAK, *Analysis of Natural Frequencies of Delaminated Composite Beams Based on Finite Element Method*, An International Journal Structural Engineering and Mechanics, Vol.4, No.3, pp.243-255, 1996.

8. S.B. TESSLER and DONG, *On a Hierarchy of Conforming Timoshenko Beam Elements*, Computer and Structure, Vol.38, pp.334-344, 1991.

9. W.M. OSTACHOWICZ and M. KRAWCZUK, *Dynamic Analysis of Delaminated Composite Beam*, Machine Vibration, Vol.3, pp.107-116, 1994.

10. M. KRAWCZUK, W. OSTACHOWICZ and A. ŻAK, *Dynamics of Cracked Composite Material Structures*, Computational Mechanics, Vol.20, pp.79-83, 1997.

11. A. ŻAK, M. KRAWCZUK and W. OSTACHOWICZ, *Numerical and Experimental Investigation of Free Vibration of Multilayer Delaminated Composite Beams and Plates*, Computational Mechanics, Vol.26, No.3, pp.309-315, 2000.

12. M. KRAWCZUK, A. ŻAK and W. OSTACHOWICZ, *Elastic Beam Finite Element with a Transverse Elasto-Plastic Crack*, Finite Elements in Analysis and Design, Vol.34, 61-73, 2000.

13. M. KRAWCZUK, A. ŻAK and W. OSTACHOWICZ, *Finite Element Model of Plate with Elasto-Plastic Through Crack*, Computers and Structures, Vol.79, pp.515-532, 2001.